Mater Renew Sustain Energy (2014) 3:21
DOI 10.1007/s40243-013-0021-2

ORIGINAL PAPER

SPS-sintered $NaTaO_3$–Fe_2O_3 composite exhibits enhanced Seebeck coefficient and electric current

Wilfried Wunderlich · Takao Mori · Oksana Sologub

Received: 13 September 2013 / Accepted: 11 December 2013 / Published online: 31 December 2013

Abstract $NaTaO_3$—50 wt% Fe_2O_3 composite ceramics showed a large Seebeck voltage of −300 mV at a temperature gradient of 650 K yielding a constant Seebeck coefficient of more than −500 μV/K over a wide temperature range. We report for the first time that spark plasma sintering (SPS) at low temperature (870 K) could maintain the short-circuit current of −80 μA, which makes this thermoelectric material a possible candidate for high-temperature applications up to 1,623 K. The reason for the good performance is the interface between Fe_2O_3 and surrounding $NaTaO_3$ perovskite. When SPS is used, constitutional vacancies disappeared and the electric conductivity increases remarkably yielding ZT of 0.016.

Keywords Thermoelectricity · Seebeck coefficient · Ceramics · Spark−plasma sintering · Interface

Introduction

The pressing problem of CO_2 increase and climate change requires the search for new energy sources such as the thermoelectric power generators (TEG), which can turn waste heat into usable electricity when operating at high temperatures. The research for new thermoelectric ceramic materials began in the last decade and Nb-doped $SrTiO_3$ [1, 2] $NaCoO_3$ [3], and $CaCoO_3$ [4] were found to have a remarkable figure-of-merit ZT. They are already successfully established in devices for high-temperature electric generators. A detailed band structure study of the perovskite-based Nb-doped $SrTiO_3$ material has emphasized the combination of large and small effective masses as the reason for the large Seebeck coefficient [5, 6]. While Co-based perovskites [7–9] have been investigated also as potential thermoelectric materials, our search for new materials yielded to the $NaTaO_3$ perovskite material, which is known as efficient photo catalyst for splitting water [10, 11] and its large effective electron mass [5].

The composite material $NaTaO_3$–Fe_2O_3 shows a large Seebeck voltage of −300 mV at a temperature gradient of $\Delta T = 650$ K with linear temperature dependence [10–15] and is stable up to 1,623 K [12, 15]. Yet its large resistivity has to be lowered for increasing the power factor and figure-of-merit. We have reported previous results on spark plasma sintering (SPS) experiments [15], where a remarkable increase in electric conductivity was achieved, but the Seebeck voltage has dropped. The conclusion was that either the interface structure or the microstructure has changed due to the high-temperature plasma, the vacuum, diffusion from the carbon crucible, or during the subsequent fast cooling and are responsible for the decrease of the Seebeck coefficient. Further findings were that composites processed from Fe_2O_3 and $NaTaO_3$, or additions of $NaFeO_3$ deteriorate the electric conductivity and yield to an insulator. The reason for the good performance of this composite material is the interface between Fe_2O_3 and $NaTaO_3$ with perovskite structure. The largest Seebeck voltage was measured when the second phase Fe_2O_3 reaches an amount of 50 mol% [10], which is just the percolation limit when the second phase starts to surround the perovskite phase $NaTaO_3$. Metallic behavior with high

W. Wunderlich (✉)
Department of Material Science, Tokai University, Hiratsuka-shi 259-1292, Japan
e-mail: wi-wunder@rocketmail.com

T. Mori · O. Sologub
Nat. Inst. Mat. Sci. (NIMS), Int. Center Mat. Nanoarchitec. (MANA), Tsukuba 305-0044, Japan

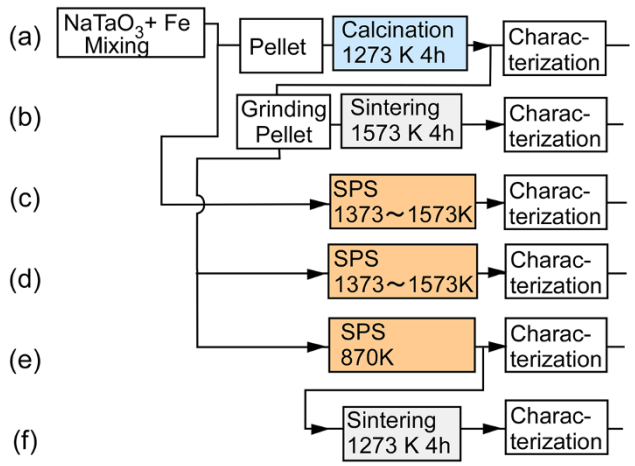

Fig. 1 The processing procedure yielded to different routes as indicated **a** calcination, **b** conventional sintering, **c** SPS at 1,373–1,573 K, **d** calcination 1,273 K in air, then SPS at 1,373–1,573 K, **e** calcination 1,273 K in air, SPS at 870 K, and **f** same as **e** with additional sintering at 1,273 K for 4 h

carrier concentration was recently found at similar $NaTaO_3/SrTiO_3$ perovskite interfaces [16].

Hence, the goal of this paper is to gain deeper insight in the materials behavior with the goal to improve both, Seebeck voltage and electric conductivity. For optimum densification, a second sintering step is required after calcination and grinding. Therefore, this paper describes processing of these composite ceramics on different routes and compare both, thermoelectric and microstructural properties of the resolved specimens.

Experimental procedure

Powders in μm size of $NaTaO_3$ and Fe (Fine Chemicals Ltd., Japan) were weighed according to the desired weight ratio of 50 mol-% Fe_2O_3 and mixed in a mortar for at least 10 min. Then the mixture was put in a steel cylinder with 15-mm diameter and cold-pressed with a stress of 50 MPa. These pellets were used in the following different synthesis methods as sketched in Fig. 1. The conventional calcination and sintering route are shown as paths (a) and (b) in Fig. 1 and details have been described in [12–14]. A sliced specimen with 10 × 2 × 2 mm dimensions was measured using the thermoelectric multi-measuring device ZEM3 (Ulvac Ltd., Japan) as described in the following section.

The next straight-forward step is to try SPS on the cold-pressed pellet [route (c) in Fig. 1] [15]. The report on such specimens showed improved resistivity, but poor Seebeck voltage [15]. The present paper focusses on SPS sintering. After calcination, the specimen were crushed, then the powder mixed again and put into a 15 mm graphite cylinder and finally attached in the Doctor Sinter 1080 SPS device (Syntex Sumitomo Heavy Industries, Ltd). Two regimes were tested and are marked as high and low temperature routes (d) and (e) in Fig. 1, namely 1,373–1,573 K and 870 K, respectively. The maximum pressure of 80 MPa was applied and kept constant, while temperature, spark plasma voltage and current were increased as described in detail in [15]. The plasma chamber was first evacuated, and then the sintering was performed at 1 atm Ar pressure. The duration of sintering was kept constant as 600 s.

The obtained specimens were characterized concerning their microstructure and composition using a Hitachi 3200-N scanning electron microscope (SEM) operated at 20 kV and equipped with an electron dispersive spectrometer (EDS, Noran Ltd.). The thermoelectric voltage was measured against nickel wires with a distance of 10 mm in a home-made device when applying a temperature difference between the micro-ceramic heater (Sakaguchi Ltd. MS 1000) up to 1,273 K, and maintaining the cold end at around 473 K, as reported elsewhere [12–14]. The electric multi-meter measurement devices (Sanwa PC510) recorded the data directly on a computer. The densities of the specimens were calculated from their mass-to-volume ratio, where the specimen dimensions were measured by a caliper.

Results and discussion

At first, a conventionally calcined and sintered specimen as described in [12] was measured for the first time by using a ZEM3. The thermoelectric measurements as displayed in Fig. 2 confirmed the relatively high resistivity, which decreases as a function of temperature. At $T = 1{,}000$ K the resistivity reached as less as 0.05 Ω m, as shown in Fig. 2a, about one order of magnitude better than previously reported values [12]. The Seebeck coefficient reaches −0.6 mV/K (Fig. 2b) and is almost constant over a wide temperature range from 600 to 1,000 K, allowing such specimen to be used as reference specimens for calibrating a measuring device. These measurements are in good agreement with previously published ones [12–14], and hence justify the validity of the Seebeck coefficient measurements under large temperature gradient at least for this materials with its constant Seebeck coefficient over a large temperature range. The power factor $S^2\,\sigma$ as displayed in Fig. 2c reaches a value of 6×10^{-6} W/m K, which is yet one or two orders of magnitude smaller than comparable oxides [1–4]. The reason is that the resistivity remains still unacceptable large as concluded from this measurement and motivates the SPS processing trial reported in the following section. When closing the open circuit with different load resistors (1–100 kΩ), the electric current was

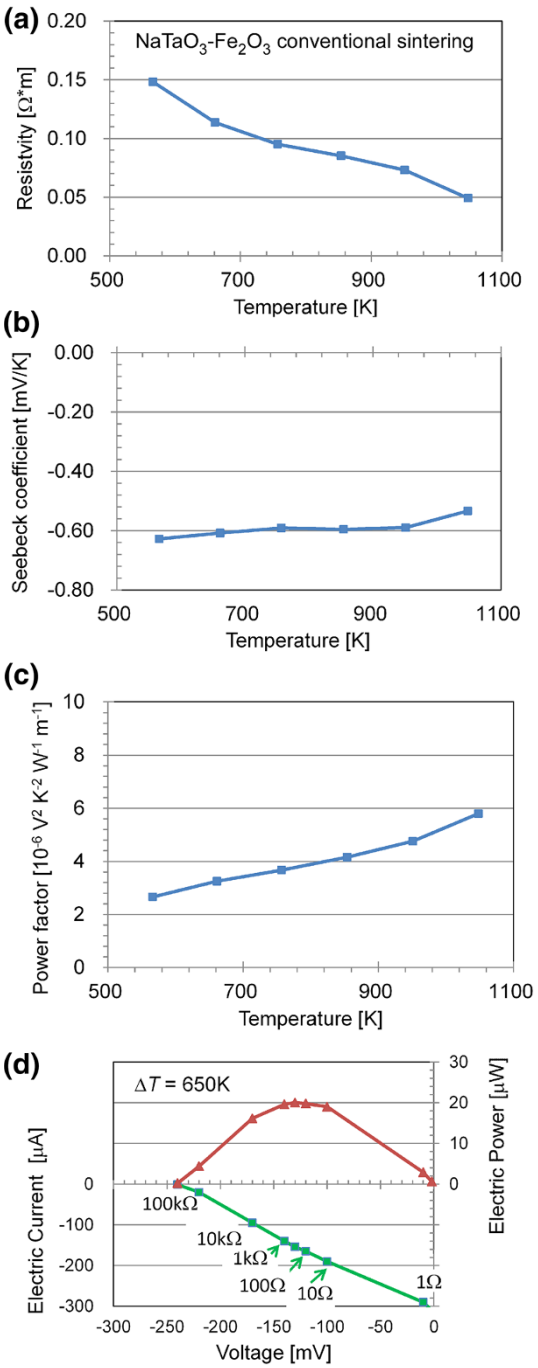

Fig. 2 Thermoelectric properties of $NaTaO_3$-50 mol% Fe_2O_3 produced by calcination and conventional sintering **a** resistivity, **b** Seebeck coefficient, **c** power factor $S^2\,\sigma$, **d** closed circuit current as a function of the Seebeck voltage and generated electric power at $\Delta T = 650$ K

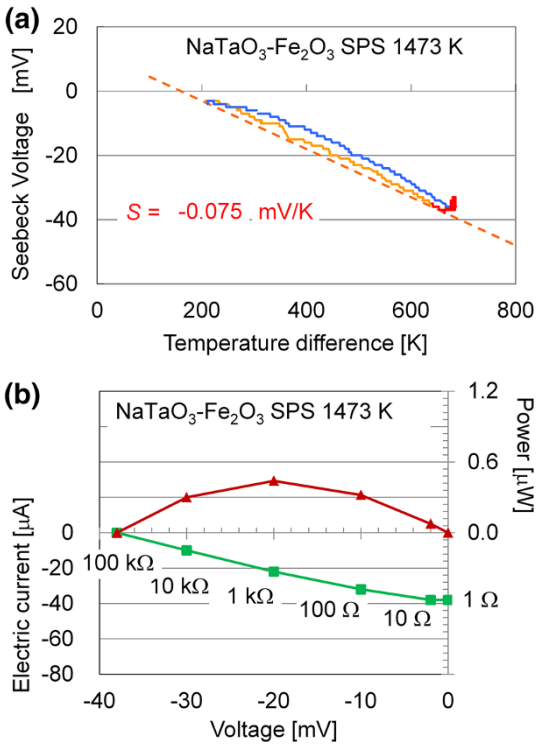

Fig. 3 **a** Seebeck voltage of a $NaTaO_3$-50 mol% Fe_2O_3 specimen, which was calcined and then SPS sintered at 1,473 K. **b** Electric current as a function of Seebeck voltage at $\Delta T = 650$ K when load resistors are applied

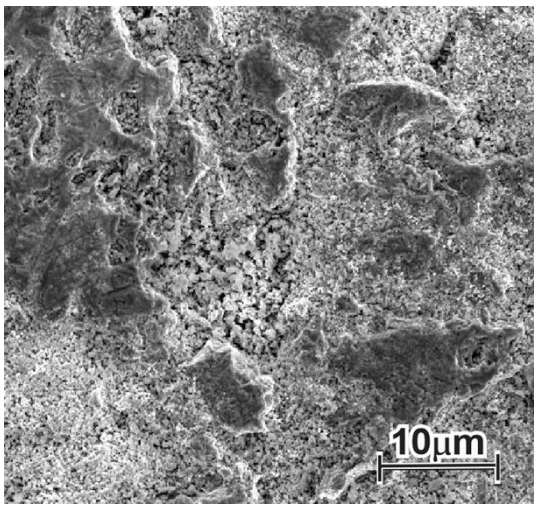

Fig. 4 Microstructure of the SPS specimen sintered at 1,473 K

measured. The maximum in this closed circuit current was −0.32 mA, and the maximum Seebeck voltage was −240 mV with a linear dependence (Fig. 2d). This relation yields at an intermediate operation point at $U = -130$ mV, $I = -154$ μA to a maximum power of $P = U \times I = 20$ μW for a temperature difference $\Delta T = 650$ K, which is still a factor of 10 below state-of-the-art oxides [3, 4]. By assuming a thermal conductivity of $\kappa = 1.7$ W/m K such as typical for comparable perovskites, we end up with a figure-of-merit in the order of ZT = 0.016, still low, but promising.

In order to improve the electric conductivity, we tried the SPS sintering at high temperatures 1,373, 1,473 and

Table 1 Density and thermoelectric properties of the $NaTaO_3$-50 mol % Fe_2O_3 composites as a function of processing method and sintering temperature

Processing method	Sinter temperature (K)	Density (kg/m^3)	Seebeck coefficient (mV/K)	Electric current (μA)	Maximal power (μW)
(a) [12]	1,273	2.55	−0.50	−50	2.5
(b) [12, 13], Fig. 1	1,473	2.82	−0.62	−320	20
(c) [15]	1,473	4.36	−0.001	−10	0.01
(d) Fig. 3	1,473	4.43	−0.075	−40	0.5
(e) Fig. 5a	870	2.88	−0.50	−10	0.1
(f) Fig. 5b	1,273	3.56	−0.50	−80	4

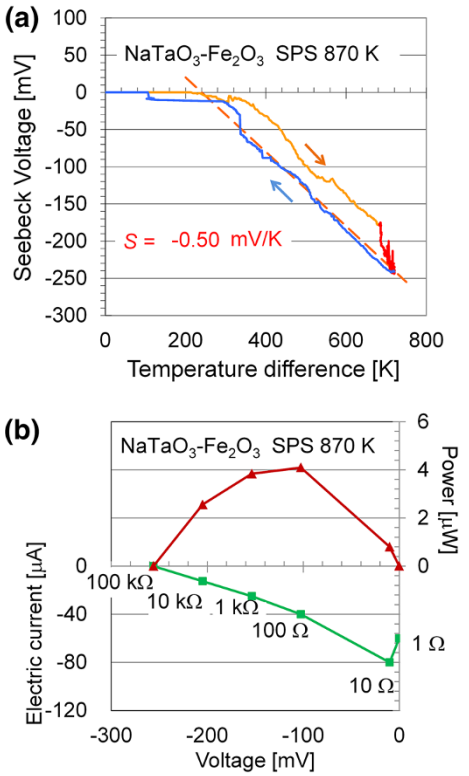

Fig. 5 Thermoelectric characterization of the $NaTaO_3$-50 mol% Fe_2O_3 calcined and **a** SPS sintered at 870 K only, and **b** sintered two times, with SPS at 870 K and 1,273 K 4 h. **a** Seebeck voltage as function of a large temperature gradient, where the *arrows* mark the heating and cooling, and the *slope* marks the Seebeck coefficient. **b** Electric current and power as a function of Seebeck voltage at $\Delta T = 650$ K, when load resistors are applied as marked

1,573 K on previously calcined specimens as sketched in Fig. 1c. The absolute value of the Seebeck voltage was reduced to −38 mV as shown in Fig. 3a, and also a lower absolute value of the closed circuit current of −40 μA (Fig. 3b). Compared to a maximum of the Seebeck coefficient of $S = -0.62$ mV/K for the conventional sintered $NaTaO_3$–Fe_2O_3 samples, the Seebeck coefficient decreased to $S = -0.075$ mV/K. The vanishing close circuit current can be explained by similar experience from a SPS sintering experiment without pre-calcining this material [15], route (c) in Fig. 1. One or more of the factors, vacuum, Ar pressure, spark plasma, the surrounding carbon container, or the fast cooling rate, are apparently bad conditions, which are deteriorating both, the Seebeck voltage and electric conductivity, probably by reducing the oxygen content or changing the interface structure.

Microstructural characterization by SEM, as shown in Fig. 4, confirmed that large pores due to insufficient compaction disappeared, but smaller pores on a sub-micrometer scale are still present in some areas. Their shape and location between Fe_2O_3 (black) and $NaTaO_3$ (white) suggest that two mechanisms are occurring; at first, the solving Fe into $NaTaO_3$ perovskite lattice and then the oxidation of Fe to Fe_2O_3, both are responsible for these pores due to unbalanced stoichiometry. Nevertheless, the density has remarkably increased compared to the conventional sintering as shown in Table 1, which compares all experiments.

In order to improve the thermoelectric properties, we have processed another sample by calcination and subsequent SPS at low temperature of 870 K according to route (e) in Fig. 1, see also Table 1. This sample maintained the large Seebeck coefficient of −0.5 mV/K (Fig. 5a). By subsequent sintering at 1,273 K 4 h [step (f)] simultaneously, a maximum current of −80 μA was measured when closing the circuit with the load of a 10 Ω resistor. This is the first time that such specimens revealed good thermoelectric performance after SPS sintering, in spite of the fact that the output power is still one order of magnitude less than that of conventional sintered specimens, as shown in Fig. 5b. The specific resistivity decreased one order of magnitude and reached 0.015 Ω m at a temperature of 1,100 K, which means the figure-of-merit is $ZT = 0.016$. This fact confirms the benefits of using SPS sintering for closing pores and increasing density. In SEM micrographs, like that shown in Fig. 6, areas with stoichiometric frustration have almost vanished. The EDX mapping confirmed the homogenous distribution of chemical elements in the dark phase, Fe_2O_3, as well as in the bright one, $NaTaO_3$.

The results of this study are summarized in Table 1, which has the same notation of processing steps as Fig. 1. While solving Fe into $NaTaO_3$ and calcination requires

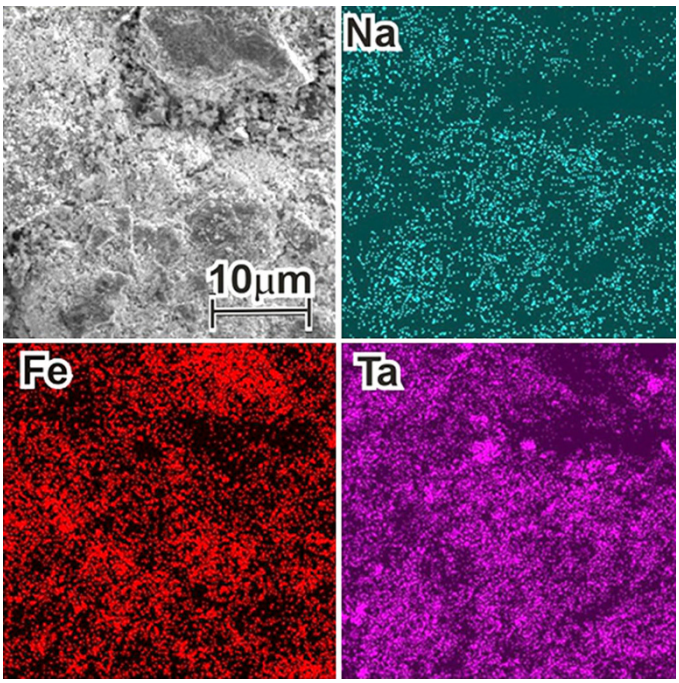

Fig. 6 Microstructure and element mapping by SEM-EDX of the specimen calcined and SPS sintered at 870 K the SPS specimen sintered at 1,473 K according to Fig.1e

slow annealing [steps (a) and (b)], densification by maintaining a large negative Seebeck coefficient was confirmed here for the first time. The large electric conductivity is explained by the enlarged densification (Table 1) due to applied pressure during SPS sintering. The shrinkage factor c defined as $c = t_f/t_0$, where t_0 and t_f are the thicknesses before and after SPS, were estimated as 0.9, constant for all SPS experiments (c–e), and no anisotropies in S or σ were found.

On the other hand, the large thermo power can only be maintained, when the specimens are sintered by SPS at relatively low temperature below 900 K with subsequent sintering in air [steps (e) and (f)]. This fact also confirmed the self-repairing ability of this composite besides the long-term stability due to the fact that thermoelectric properties improved after each sintering cycle [12, 13]. Further investigations should confirm the detailed mechanism why a large negative Seebeck coefficient and a fairly large electric conductivity are achieved at the same time. The fact that the optimum composition fits well to the percolation composition [12], where the volume fraction of both phases is equal, as well as results from recent reports [2, 16] indicate that a confined two-dimensional electron gas (2DEG) at the heterogeneous interface is the reason for the good performance of this composite. Further improvement of ZT is expected from nano-scaled composites or super lattices or by finding suitable co-dopants.

Conclusions

The results of this SPS study on the $NaTaO_3$–Fe_2O_3 composite material confirmed the following facts.

(1) For the first time, we could achieve a large negative Seebeck voltage of this n-type thermoelectric and closed circuit current with remarkable power output by substantially decreasing the SPS sintering temperature from 1,273 to 870 K.
(2) The densities of the SPS-processed specimens were much higher than the cold-pressed specimens with fewer pores and cracks, leading to a significantly lower electrical resistivity.
(3) Sub-micrometer sized pores due to constitutional frustration almost disappeared confirming the homogeneous microstructure after calcination and subsequent SPS sintering at low temperature. While densification improved the electric conductivity significantly, the large thermo power can only be maintained by slow heating in air, low SPS sintering temperature and subsequent sintering at high temperature.

References

1. Ohta, S., Nomura, T., Ohta, H., Hosono, H., Koumoto, K.: Large thermoelectric performance of heavily Nb-doped $SrTiO_3$ epitaxial film at high temperature. Appl. Phys. Lett. **87**, 092108 (2005). doi:10.1063/1.2035889
2. Ohta, H., Kim, S., Mune, Y., Mizoguchi, T., Nomura, K., Ohta, S., Nomura, T., Nakanishi, Y., Ikuhara, Y., Hirano, M., Hosono,

H., Koumoto, K.: Giant thermoelectric Seebeck coefficient of a two-dimensional electron gas in $SrTiO_3$. Nat. Mater. **6**, 129 (2007). doi:10.1038/nmat1821
3. Terasaki, I., Sasago, Y., Uchinokura, K.: Large thermoelectric power in $NaCo_2O_4$ single crystals. Phys. Rev. B **56**, R12685 (1997). doi:10.1103/PhysRevB.56.R12685
4. Funahashi, R., Matsubara, I., Ikuta, H., Takeuchi, T., Mizutani, U., Sodeoka, S.: An Oxide single crystal with high thermoelectric performance in air. Jpn. J. Appl. Phys. **39**, L1127 (2000). doi:10.1143/JJAP.39.L1127
5. Wunderlich, W., Ohta, H., Koumoto, K.: Enhanced effective mass in doped $SrTiO_3$ and related perovskites. Phys. B **404**, 2202 (2009). doi:10.1016/j.physb.2009.04.012
6. Shirai, K., Yamanaka, K.: Mechanism behind the high thermoelectric power factor of $SrTiO_3$ by calculating the transport coefficients. J. Appl. Phys. **113**, 053705 (2013). doi:10.1063/1.4788809
7. Tomes, P., Robert, R., Trottmann, M., Bocher, L., Aguirre, M.H., Bitschi, A., Hejtmanek, J., Weidenkaff, A.: Synthesis and characterization of new ceramic thermoelectrics implemented in a thermoelectric oxide module. J. Elec. Mat. **39**(9), 1696 (2010). doi:10.1007/s11664-010-1214-4
8. Wunderlich, W., Fujiwara, H.: The difference between thermo- and pyroelectric Co-based RE-(=Nd, Y, Gd, Ce)-oxide composites measured by high-temperature gradient. J. Electron. Mater. **40**(2), 127–133 (2011). doi:10.1007/s11664-010-1420-0
9. Wunderlich, W.: Large Seebeck voltage of Co, Mn, Ni, Fe-ceramics. Adv. Ceram. Sci. Eng. (ACSE) 2(1), 9–15 (2013). http://www.acse-journal.org/Download.aspx?ID=5579
10. Kato, H., Kudo, A.: New tantalate photocatalysts for water decomposition into H and O_2. Chem. Phys. Lett. **295**, 487–492 (1998). doi:10.1016/S0009-2614(00)01220
11. Kudo, A., Kato, H.: Effect of lanthanide-doping into $NaTaO_3$ photocatalysts for efficient water splitting. Chem. Phys. Lett. **331**, 373–377 (2000)
12. Wunderlich, W.: $NaTaO_3$ composite ceramics—a new thermoelectric material for energy generation. J Nucl. Mat. **389**(1), 57–61 (2009). doi:10.1016/j.jnucmat.2009.01.007
13. Wunderlich, W., Soga, S.: Microstructure and Seebeck voltage of $NaTaO_3$ composite ceramics with additions of Mn, Cr, Fe or Ti. J. Ceram. Proc. Res. **11**, 233–236 (2010)
14. Wunderlich, W., Baufeld, B.: Development of thermoelectric materials based on NaTaO3—composite ceramics. In: Wunderlich, W. (ed.) Ceramic materials, pp. 1–27. Intech Publisher, London (2010). doi:10.5772/243
15. Wunderlich, W., Mori, T., Sologub, O., Baufeld, B.: SPS-sintering of $NaTaO_3$–Fe_2O_3 composites. J. Aust. Ceram. Soc. **47**(2), 57–60 (2011)
16. Nazir, S., Schwingenschlögl, U.: High charge carrier density at the NaTaO3/SrTiO3 hetero-interface. Appl. Phys. Lett. **99**, 073102 (2011). doi:10.1063/1.3625951